Dielectrophoretic Movement of Cell around Surface Electrodes in Flow Channel

Yusuke TAKAHASHI, Shigehiro HASHIMOTO, Manabu WATANABE
Biomedical Engineering, Department of Mechanical Engineering,
Kogakuin University, Tokyo, 163-8677, Japan
http://www.mech.kogakuin.ac.jp/labs/bio/

ABSTRACT

A micro flow channel with the surface electrodes has been designed to detect the dielectrophoretic movement of a biological cell. The surface electrodes of titanium (thickness of 200 nm) were formed along the edges of the flow channel by the photolithography technique. At the one of the edges, the tip angle of the triangle shape of the surface electrode is 0.26 rad. The other flat edge is the reference electrode. The rectangular periodic electrical stimulation (0.01 ms, or 0.001 ms of period) was applied between the surface electrodes. The suspension of C2C12 (mouse myoblast cell line originated with cross-striated muscle of C3H mouse) was introduced into the flow channel, and the flow rate was controlled by the pressure head between the inlet port and the outlet port. The experiment shows that the velocity of the cell is accelerated along the electric field during the flow through the flow channel.

Keywords: Biomedical Engineering, Dielectrophoresis, Titanium, Surface Electrode and C2C12.

1. INTRODUCTION

The movement of a biological cell suspended in the medium is governed by several factors: electric force, Van der Waals force, affinity of surface, and pressure. Various methods have been applied to control the movement of cells *in vitro*: micro slit [1], flow [2, 3], gravitational field [4], electric field [5], and magnetic field [6, 7]. These methods have the potential to contribute to several applications of manipulation of cells: arrangement of cells to make a tissue [8], sorting of cells [1, 9-12], and measurement of the character of cells.

Movement of a charged particle depends on the electric field. The effect is applied to the electrophoresis device [13]. When a particle is subjected to a non-uniform electric field, a force is exerted even on an uncharged particle, because the polarization generates in the particle. The phenomenon is called dielectrophoresis, which depends on the several parameters: the electrical property of the particle, shape and size of the particle, the electrical property of the medium, and frequency of the electric field [14-23].

Electrophoresis is a phenomenon, in which a particle moves due to the Coulomb force between the charge of the particle and the electric field. Dielectrophoresis, on the other hand, is a phenomenon, in which a particle moves due to the interaction between the electric field and the charge induced in a neutral particle, when the particle is placed in a non-uniform electric field. The force of dielectrophoresis is calculated by the equivalent dipole moment method.

$$F = \pi \varepsilon_m r^3 Re\,[K(\omega)]\ \nabla E^2 \quad (1)$$

In Eq. 1, r is the radius of the particle, ε_m is the dielectric constant of the surrounding medium, and E is the maximum value of the electric field. $Re\,[K(\omega)]$ represents the real part of the function expressed by the following equation.

$$K(\omega) = (\varepsilon_p^* - \varepsilon_m^*) / (\varepsilon_p^* + 2\,\varepsilon_m^*) \quad (2)$$

In Eq. 2, ε_p^* is the complex dielectric constant of the particle, ε_m^* is the complex dielectric constant of the solution.

In the present study, the behavior of a biological cell around the surface electrode in the flow channel has been observed *in vitro*.

2. METHODS

Surface Electrode

The titanium film was used for the surface electrode. Titanium was coated on the glass plate (38 mm × 26 mm × 1 mm, Matsunami Glass Ind., Ltd., Japan). The thickness of the coating is 200 nm.

The tip angle of the triangle shape of the one of the surface electrodes is 0.26 rad. The other reference electrode has a flat edge. The distance between electrodes (d) is 0.5 mm.

Deposition of Titanium

Before the deposition of titanium, the surface of the glass plate was hydrophilized by the oxygen (30 cm^3/min, 0.1 Pa) plasma ashing at 100 W for five minutes by a reactive ion etching system (FA-1, Samco International, Kyoto, Japan). Titanium was deposited on the surface of the glass plate with 200 nm thickness in the spattering system (back pressure < 9×10^{-4} Pa, 100W, 0.5 Pa, 8 min, L-210S-FH Canon Anelva Corporation, Kawasaki, Japan).

Photomask for Triangular Electrode

To improve affinity between titanium and photoresist material, HMDS (hexamethyldisilazane: Tokyo Chemical Industry Co., Ltd., Tokyo) was coated on the glass plate at 3000 rpm for 30 seconds by using a spin coater. The positive photoresist material of OFPR-800LB (Tokyo Ohka Kogyo Co., Ltd, Tokyo, Japan) was coated on HMDS with the spin coater (at 7000 rpm for 60 seconds) (Fig. 1). The photoresist was baked in the oven with two processes: at 338 K for one minute, and at 368 K for three minutes.

The pattern of the electrode was drawn on the mask four times with a laser drawing system (DDB-201K-KH, Neoark Corporation, Hachioji, Japan). To control the dimension of the pattern on the photomask with the laser drawing system, the

parameters were selected as follows: the voltage of 2.3 V, the velocity of 0.08 mm/s, and the acceleration of 0.5 mm/s^2. The photoresist was developed with tetra-methyl-ammonium hydroxide (NMD-3, Tokyo Ohka Kogyo Co., Ltd., Kawasaki, Japan) for three minutes, rinsed with the distilled water, and dried by the spin-dryer with nitrogen gas (SF-250, Japan Create Co., Ltd., Tokorozawa, Japan).

The titanium-coated plate was etched with the plasma gas using RIE-10NR (Samco International, Kyoto, Japan). For etching, the gas of SF_6 (50 cm^3/min at 1013 hPa) with Ar (50 cm^3/min at 1013 hPa) was applied at 100 W at 4 Pa for five minutes. The residual OFPR-800LB was removed with acetone (Fig. 2).

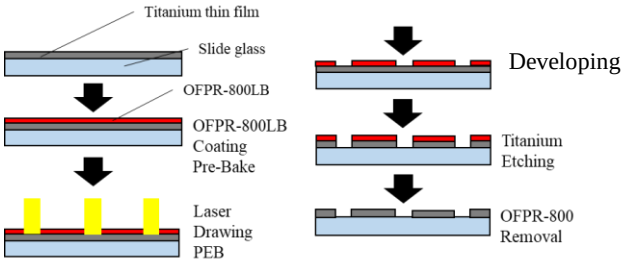

Fig. 1: Photolithography process for photomask.

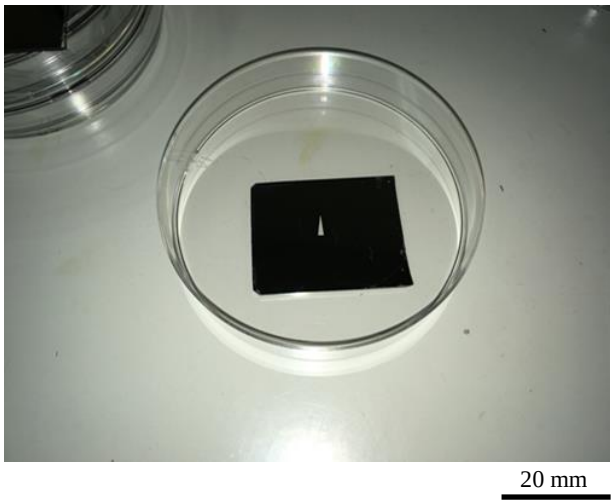

Fig. 2: Photomask for triangular electrode.

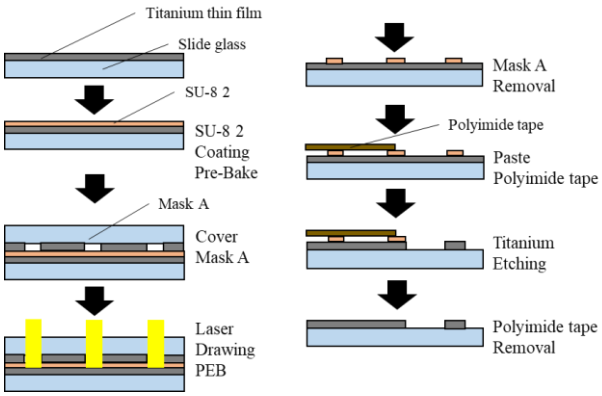

Fig. 3: Photolithographic process of surface electrode.

Surface Electrodes

The titanium-coated glass plate was hydrophilized with oxygen (30 cm^3/min, 0.1 Pa) by plasma ashing at 100 W for five minutes by a reactive ion etching system (FA-1) (Fig. 3). The negative photoresist material of low viscosity (SU-8 2: Micro Chem Corp., MA, USA) was coated on the glass plate with the spin coater (at 7000 rpm for 60 seconds). The photoresist was baked in the oven at 368 K for five minutes.

The photomask was mounted on the surface of SU-8 2, and the photoresist was exposed to the UV light through the mask in the mask aligner (M-1S, Mikasa Co. Ltd., Japan) at 15 mW/cm^2 for 12 s. The photoresist was baked in the oven at 368 K for five minutes. The photoresist was developed with SU-8 Developer (Micro Chem Corp., MA, USA) for five minutes.

The glass surface with the micro pattern was rinsed with IPA (2-propanol, Wako Pure Chemical Industries, Ltd.) for one minute, and with pure water for one minute. The surface was dried by the spin-dryer: at 300 rpm for 30 s with the distilled water, and at 1100 rpm for 30 s with N_2 gas.

Before etching, the areas at the bands of both ends were covered with the polyimide tapes to leave the part of titanium coating for electrodes. The titanium coated plate was etched with the plasma gas using RIE-10NR. For etching, the gas of SF_6 (50 cm^3/min at 1013 hPa) with Ar (50 cm^3/min at 1013 hPa) was applied at 100 W at 4 Pa for ten minutes. After etching, the polyimide tapes were removed (Fig. 4).

Flow Channel

The wall of flow channel was made of polydimethylsiloxane (PDMS). The polyimide tape (0.055 mm thickness, 10 mm width) was pasted at the center of the glass plate, and cut into the rectangular shape (1 mm width, 25 mm length) by the ultra-short pulse laser (IFRIT, Cyber Laser Inc., Tokyo, Japan) to make groove for the flow channel.

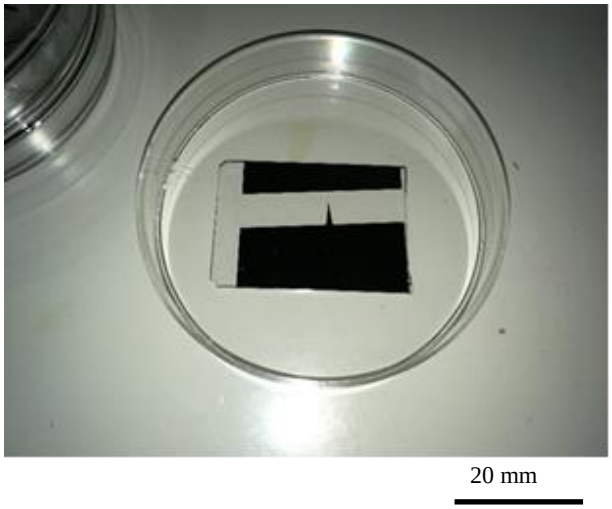

Fig. 4: Surface electrodes.

Fig. 5: Flow channel with surface electrodes.

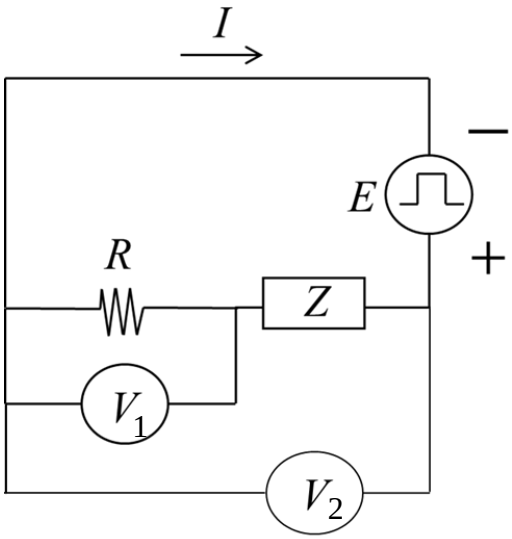

Fig. 6: Electric circuit: electric stimulation (*E*) applied to flow channel (*Z*): V_1, voltage between terminals of resistance *R*: V_2, voltage between terminals of stimulator *E*: *I*, current.

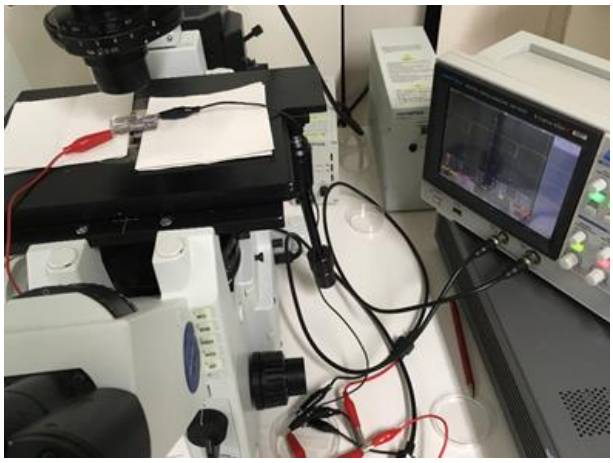

Fig. 7: Experimental system.

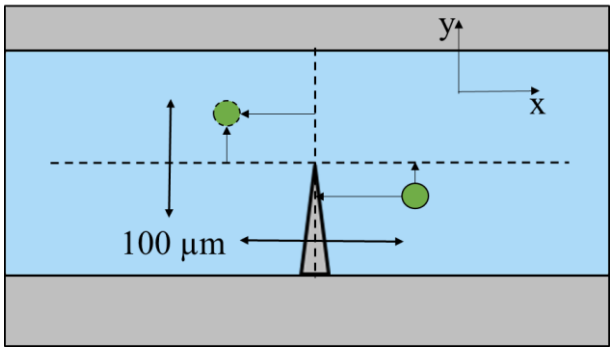

Fig. 8: Coordinates for tracing of cell: flow from left to right.

After the slide glass plate was enclosed with the peripheral wall of polyimide tape, PDMS (Sylgard 184 Silicone Elastomer Base, Dow Corning Corp., MI, USA) of 4.4 cm^3 was poured on the plate together with the curing agent (Sylgard 184 Silicone Elastomer Curing Agent, Dow Corning Corp., MI, USA). The volume ratio of PDMS to curing agent is ten to one. After degassing, PDMS was baked at 373 K for one hour in an oven (DX401, Yamato Scientific Co., Ltd).

Two holes (diameter; 5 mm) with the interval of 20 mm were punched by a punching tool (trepan BF-50F, Kai Industries Co., Ltd., Gifu, Japan) to make the inlet and the outlet. The both ends were cut to expose the ends of surface electrodes to make the electric connection. The baked plate of PDMS (4 mm thickness) was peeled off from the slide glass plate.

The upper plate of PDMS was stuck on the lower plate of the glass with the surface electrodes to make the flow channel (Fig. 5). A rectangular parallelepiped channel (25 mm length × 1 mm width × 0.05 mm height) is formed between the upper and the lower plates.

Electric Stimulation

The electric stimulation (*E*) of the rectangular cyclic wave (0.1 MHz, or 1 MHz; V = ±2.5 V, ±5 V, or ±7.5 V) was generated with an electric stimulator (WS8102, Toyo Corporation, Japan). The stimulator was connected to the titanium film electrode, and the electric signal was introduced to the medium of cells (*Z*). An electrical resistance (*R*) of 1 kΩ is inserted in series between the electrode and the stimulator. The electric signal between the terminals of the resistance (V_1) is monitored by an oscilloscope during electric stimulation applied between the titanium surface electrodes (Fig. 6).

Cell

C2C12 (mouse myoblast cell line originated with cross-striated muscle of C3H mouse) was used in the test. D-MEM (Dulbecco's Modified Eagle Medium) containing 10% FBS (Fetal Bovine Serum) and 1% penicillin/streptomycin was used as the medium.

Before the flow test, the inner surface of the flow channel was hydrophilized by the oxygen (30 cm^3/min, 0.1 Pa) plasma ashing for one minute at 100 W by the reactive ion etching system (FA-1), and prefilled with the phosphate buffer solution.

Before the flow test, the cells were exfoliated from the plate of the culture dish with trypsin, and suspended in the medium.

The suspension of cells was poured at the inlet of the flow channel. The flow occurs by the pressure difference between the inlet and the outlet, which was kept by the gravity level of the medium (< 3 mm).

Each cell passing between the electrodes was observed by the inverted phase-contrast microscope (IX71, Olympus Co., Ltd., Tokyo), and recorded by the camera (DSC-RX100M4, Sony Corporation, Japan), which is set at the eyepiece of the microscope (Fig. 7). The movement of the cell was analyzed by "Kinovea (Ver. 8.23, Commons Attribution)" at the video images: 30 frames per second. To trace the movement of the cell, the coordinates are defined as that in Fig. 8. The origin is adjusted at the tip of the triangular electrode.

3. RESULTS

Fig. 9 exemplifies tracings of the voltage of electric stimulation of rectangular cyclic waves. The lower purple wave shows V_1, and upper yellow waves shows V_2. The frequencies are 0.1 MHz (Fig. 9a) and 1 MHz (Fig. 9b). At higher frequencies, the voltage alternates before the saturation of the voltage.

Fig. 10 exemplifies microscopic images at the stimulation of 1 MHz (± 7.5 V). C2C12 (marked in circle) approaches to the tip of the electrode (upper left), moves through the tip of the electrode (upper right, and lower left), and moves away from the tip (lower right).

In Figs. 11-12, the coordinate of x corresponds to the flow direction, and the coordinate of y corresponds to the direction perpendicular to x. The location of the tip of the triangular electrode is zero of x.

Fig. 11 exemplifies tracings of movement of C2C12 passing through adjacent to the tip of the electrode. Data were collected at 0.1 MHz (Fig. 11a: 5 V_{P-P}) and at 1 MHz (Fig. 11b: 15 V_{P-P}), respectively. Fig. 11b shows apparent shift of the movement of C2C12 adjacent to the tip of the electrode.

Fig. 12 shows the velocity of C2C12: x component (blue), and y component (red): the cell moves along flow from left (negative x) to right (positive x). The experimental condition of "frequency and amplitude" are "0.1 MHz, ±2.5 V" (Fig. 12a), "0.1 MHz, ±5 V" (Fig. 12b), "0.1 MHz, ±7.5 V" (Fig. 12c), "1 MHz, ±2.5 V" (Fig. 12d), "1 MHz, ±5 V" (Fig. 12e), "1 MHz, ±7.5 V" (Fig. 12f), respectively. In several conditions, not only the y component of the velocity, but also the x component of the velocity varies adjacent to the tip of the electrode. At ±2.5 V (Figs. 12a & 12d), the x component of the velocity of C2C12 is not shifted after passing through the electrode.

When C2C12 passes adjacent to the tip of the electrode (distance between electrodes, 0.49 mm) at the electric stimulation of rectangular cyclic voltage of 15 Vp-p at 1 MHz, the velocity of C2C12 of 0.023 mm diameter is accelerated to that of 1.5 times. The moving direction is diagonally shifted to 0.07 mm per millimeter downstream.

The amplitude of the electric rectangular current of ± 0.023 mA, for example, is calculated by the amplitude of the electric rectangular voltage of ± 23 mV between terminals of the resistance of 1 kΩ.

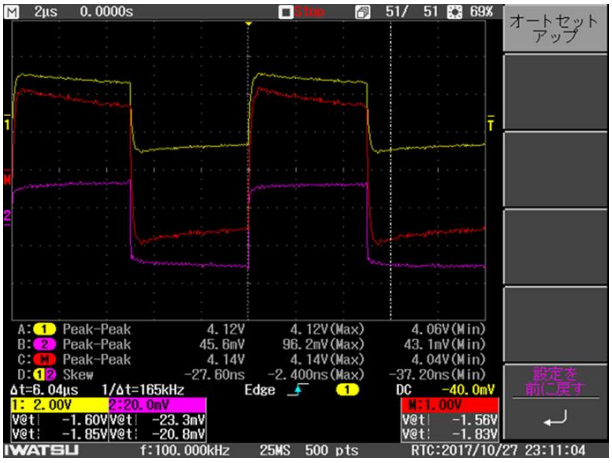

Fig. 9a: Tracings of voltage of electric stimulation: V_1 (lower, purple), V_2 (upper, yellow): 0.1 MHz, ± 5 V).

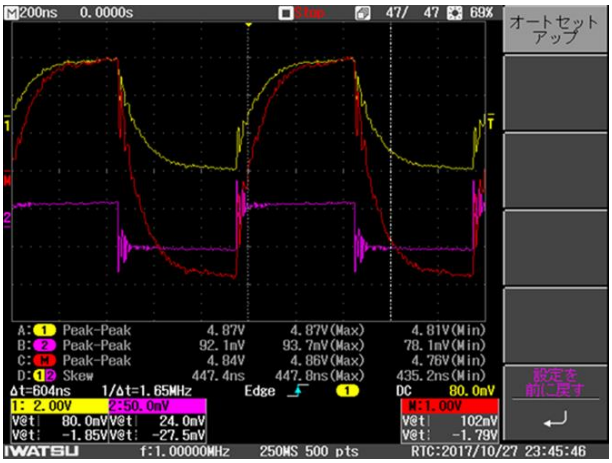

Fig. 9b: Tracings of voltage of electric stimulation: V_1 (lower, purple), V_2 (upper, yellow): 1 MHz, ± 7.5 V.

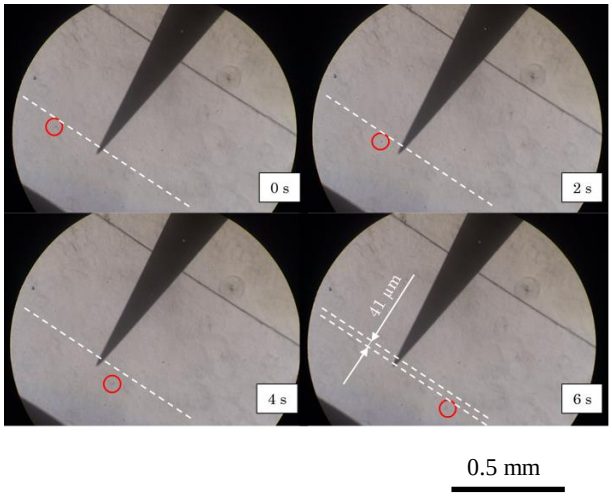

Fig. 10: C2C12 (marked in circle) approaches to the tip of the electrode (upper left), moves away from the tip (lower right): 1 MHz, ±7.5 V.

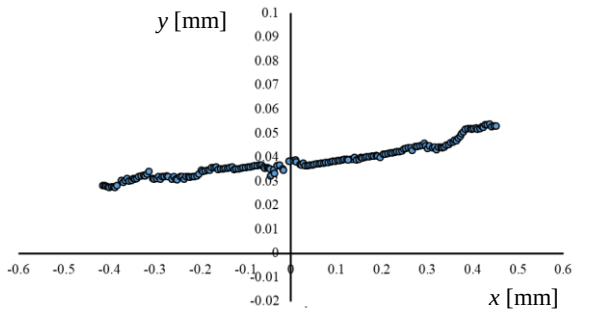

Fig. 11a: Tracings of movement of C2C12: *x* coordinate (flow direction), *y* coordinate (perpendicular to *x*), origin (tip of electrode): 0.1 MHz, ±2.5 V.

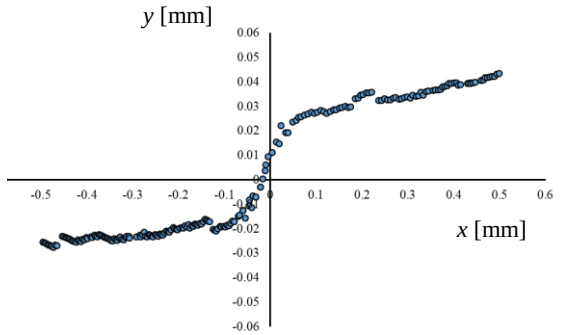

Fig. 11b: Tracings of movement of C2C12: *x* coordinate (flow direction), *y* coordinate (perpendicular to *x*), origin (tip of electrode): 1 MHz, ±7.5 V.

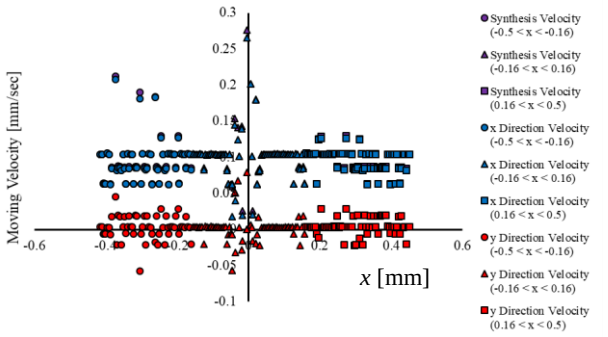

Fig. 12a: Velocity of C2C12: *x* component (blue), and *y* component (red): cell moves along flow from left (negative *x*) to right (positive *x*): 0.1 MHz, ±2.5 V.

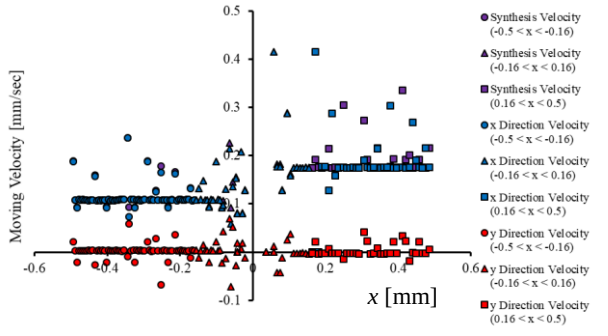

Fig. 12b: Velocity of C2C12: *x* component (blue), and *y* component (red): cell moves along flow from left (negative *x*) to right (positive *x*): 0.1 MHz, ± 5 V.

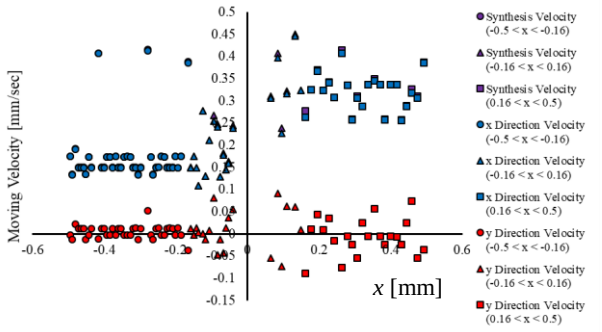

Fig. 12c: Velocity of C2C12: *x* component (blue), and *y* component (red): cell moves along flow from left (negative *x*) to right (positive *x*): 0.1 MHz, ± 7.5 V.

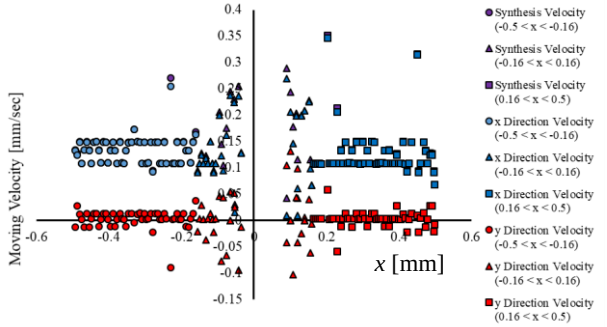

Fig. 12d: Velocity of C2C12: *x* component (blue), and *y* component (red): cell moves along flow from left (negative *x*) to right (positive *x*): 1 MHz, ±2.5 V.

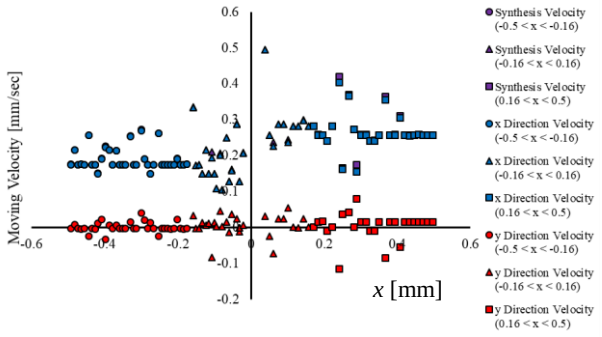

Fig. 12e: Velocity of C2C12: *x* component (blue), and *y* component (red): cell moves along flow from left (negative *x*) to right (positive *x*): 1 MHz, ± 5 V.

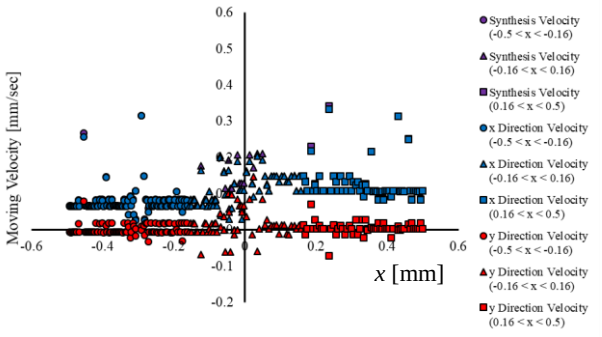

Fig. 12f: Velocity of C2C12: *x* component (blue), and *y* component (red): cell moves along flow from left (negative *x*) to right (positive *x*): 1 MHz, ± 7.5 V.

4. DISCUSSION

The maximum shift distance of the cell has been very small (71 μm) in the present experiment. If the shift movement of the cell adjacent to the tip of the electrode is expanded downstream due to the inertial movement, the method can be applied to the cell sorting. For the continuous movement of the downstream cell, it is necessary to consider the relationship between the stream line of the cell and the position of the side wall of the flow channel.

In another way, the accumulated shift by the multiple electrodes might expand the shift movement of the cell [14]. In the present study, the dielectrophoretic movement of the cell was attempted to be observed by the optical microscope. The dielectrophoretic movement might be enhanced by the shorter distance between electrodes. The electrodes arrangement with the shorter distance has not been designed, since the electrodes are not optically transparent in the present study.

The shift might depend on the passing route of the cell. The dielectrophoretic effect might be highest adjacent to the tip of the electrode. The shift might depend on the size of the particle. The voltage between electrodes higher than 15 V might enlarge the shift. The higher voltage or current, however, can cause electrolysis at the tip of the electrode. The amplitude of the electric stimulation has been limited within the threshold value to prevent electrolysis in the present study.

Figs. 10-12 show the movement in the *x-y* plane. Since the height of the channel is 0.055 mm, the movement in the direction (*z*) perpendicular to the flow is very small. The movement of cells between surface electrodes depends on the morphology of surface electrodes (the angle of the tip), which relates to non-uniformity of electric field [14]. Dielectrophoresis of cell depends on the asymmetric figure of electrodes.

The higher gradient of electric field with non-uniformity is necessary to enlarge the movement of cells around the electrode. The smaller angle of the tip of the electrode might generate non-uniform electric fields, which accelerate dielectrophoresis.

.

In the previous study, dielectrophoresis has been applied to the biological cell manipulation techniques [14-23]. The micro-grooves were used for trapping of flowing cells in the previous study [9].

5. CONCLUSION

A micro flow channel with the surface electrodes of titanium has been designed to detect the dielectrophoretic movement of a biological cell, and has successfully manufactured by photolithography technique. One side of the electrodes has a sharp triangular edge. The behavior of the biological cell around the surface electrode in the flow channel has been observed *in vitro*. The rectangular cyclic electric stimulation (0.1 MHz, or 1 MHz) was applied to the flow of the suspension of C2C12 (mouse myoblast cell line) between the surface electrodes. The dielectrophoretic movement of C2C12 was detected at the microscope images by the electric stimulation through the surface electrodes during the flow along the channel.

6. ACKNOWLEDGMENT

This work was supported by a Grant-in-Aid for Strategic Research Foundation at Private Universities from the Japanese Ministry of Education, Culture, Sports and Technology.

REFERENCES

[1] Y. Takahashi, S. Hashimoto, H. Hino and T. Azuma, "Design of Slit between Micro Cylindrical Pillars for Cell Sorting", **Journal of Systemics, Cybernetics and Informatics**, Vol. 14, No. 6, 2016, pp. 8-14.

[2] S. Hashimoto, F. Sato, H. Hino, H. Fujie, H. Iwata and Y. Sakatani, "Responses of Cells to Flow in Vitro", **Journal of Systemics Cybernetics and Informatics**, Vol. 11, No. 5, 2013, pp. 20-27.

[3] S. Hashimoto and M. Okada, "Orientation of Cells Cultured in Vortex Flow with Swinging Plate in Vitro", **Journal of Systemics Cybernetics and Informatics**, Vol. 9, No. 3, 2011, pp. 1-7.

[4] S. Hashimoto, H. Hino and T. Iwagawa, "Effect of Excess Gravitational Force on Cultured Myotubes in Vitro", **Journal of Systemics Cybernetics and Informatics**, Vol. 11, No. 3, 2013, pp. 50-57.

[5] S. Hashimoto, F. Sato, R. Uemura and A. Nakajima, "Effect of Pulsatile Electric Field on Cultured Muscle Cells in Vitro", **Journal of Systemics Cybernetics and Informatics**, Vol. 10, No. 1, 2012, pp. 1-6.

[6] S. Hashimoto and K. Tachibana, "Effect of Magnetic Field on Adhesion of Muscle Cells to Culture Plate", **Journal of Systemics Cybernetics and Informatics**, Vol. 11, No. 4, 2013, pp. 7-12.

[7] M. Heijazian, W. Li and N.T. Nguyen, "Lab on a Chip for Continuous-flow Magnetic Cell Separation", **Lab on a Chip**, Vol. 15, No. 4, 2015, pp. 959-970.

[8] Y. Takahashi, S. Hashimoto, H. Hino and T. Takeda, "Electric Stimulation for Acceleration of Cultivation of Myoblast on Micro Titanium Coil Spring", **Proc. 20th World Multi-Conference on Systemics Cybernetics and Informatics**, Vol. 2, 2016, pp. 153-158.

[9] Y. Takahashi, S. Hashimoto, H. Hino, A. Mizoi and N. Noguchi, "Micro Groove for Trapping of Flowing Cell", **Journal of Systemics, Cybernetics and Informatics**, Vol. 13, No. 3, 2015, pp. 1-8.

[10] S.M. McFaul, B.K. Lin and H. Ma, "Cell Separation Based on Size and Deformability Using Microfluidic Funnel Ratchets", **Lab on a Chip**, Vol. 12, 2012, pp. 2369-2376.

[11] A. Tabll and H. Ismail, "The Use of Flow Cytometric DNA ploidy analysis of liver biopsies in liver cirrhosis and hepatocellular carcinoma", **Journal of World's Largest Science Technology & Medicine**, 2011, pp. 88-107.

[12] H. Tsutsui and C.M. Ho, "Cell Separation by Non-inertial Force Fields in Microfluidic Systems", **Mechanics Research Communications**, Vol. 36, 2009, pp. 92-103.

[13] X. Xuan, B. Xu and D. Li, "Accelerated Particle Electrophoretic Motion and Separation in Converging-diverging Microchannels", **Analytical Chemistry**, Vol. 77, No. 14, 2005, pp. 4323-4328.

[14] Y. Takahashi, S. Hashimoto, R. Yamauchi, H. Hino and T. Yasuda, "Myoblast Behavior around Surface Electrodes in Flow Channel", **Proc. 21st World Multi-Conference on Systemics Cybernetics and Informatics**, Vol. 2, 2017, pp. 251-256.

[15] P.R.C. Gascoyne, X.B. Wang, Y. Huang and F.F. Becker, "Dielectrophoretic Separation of Cancer Cells from Blood", **IEEE Transactions on Industry Applications**, Vol. 33, No. 3, 1997, pp. 670-678.

[16] K.V. Kaler and T.B. Jones, "Dielectrophoretic Spectra of Single Cells Determined by Feedback-controlled Levitation", **Biophysical Journal**, Vol. 57, No. 2, 1990, pp. 173-182.

[17] Y. Wakizaka, M. Hakoda and N. Shiragami, "Effect of Electrode Geometry on Dielectrophoretic Separation of Cells", **Biochemical Engineering Journal**, Vol. 20, No. 1, 2004, pp. 13-19.

[18] I. Doh and Y.H. Cho, "A Continuous Cell Separation Chip Using Hydrodynamic Dielectrophoresis (DEP) Process", **Sensors and Actuators A: Physical**, Vol. 121, No. 1, 2005, pp. 59- 65.

[19] Y. Kang, D-D. Li, S.A. Kalams and J.E. Eid, "DC-Dielectrophoretic Separation of Biological Cells by Size", **Biomedical Microdevices**, Vol. 10, No. 2, 2008, pp. 243-249.

[20] H. Imasato and T. Yamakawa, "Measurement of Dielectrophoretic Force by Employing Controllable Gravitational Force", **Journal of Electrophoresis**, Vol. 52, No. 1, 2008, pp. 1-8.

[21] H. Shafiee, J.L. Caldwell, M.B. Sano and R.V. Davalos, "Contactless Dielectrophoresis: a New Technique for Cell Manipulation", **Biomedical Microdevices**, Vol. 11, No. 5, 2009, pp. 997-1006.

[22] B. Yafouz, N.A. Kadri and F. Ibrahim, "Dielectrophoretic Manipulation and Separation of Microparticles Using Microarray Dot Electrodes", **Sensors**, Vol. 14, No. 4, 2014, pp. 6356-6369.

[23] B.H. Lapizco-Encinas, B.A. Simmons, E.B. Cummings and Y. Fintschenko, "Dielectrophoretic Concentration and Separation of Live and Dead Bacteria in an Array of Insulators", **Analytical Chemistry**, Vol. 76, No. 6, 2004, pp. 1571-1579.